Studies of vanadium and vanadium oxide based nanocomposite structures

V. PRILEPOV, P. GASHIN, M. POPESCU[a], V. ZALAMAI[b], D. SPOIALA, P.KETRUSH, N.NASEDCHINA
Moldova State University, 60 A. Mateevici Str., Chisinau, MD-2009, Republic of Moldova
[a]National Institute of Materials Physics, 105 bis Atomistilor Str., P.O. Box MG 7, RO-77125 Măgurele, Romania
[b]Institute of Applied Physics, Academy of Sciences of Moldova, 5 Academiei Str., Chisinau, MD-2028, Republic of Moldova

The results of the surface morphology studies as well as optical and electrical properties of nano-dimensional vanadium oxide composite structures deposited on various substrates- silica, glass substrates covered by conducting layer of SnO_2, pure pyroceramics plates and the same covered by Al_2O_3, SiO_2, Ta_2O_5 layers are presented. According to Raman spectroscopy results the thin film structure obtained on quartz corresponds to the α-V_2O_5 orthorhombic phase. In contrast with this the Raman spectra of V_2O_5 films obtained on pyroceramics substrates, passivated by Al_2O_3, Ta_2O_5, SiO_2 oxides, do not appear clearly marked narrow lines which indicate their amorphous character. The investigation of the optical properties of the fabricated layers in the spectral range of 200-1000 nm had revealed the presence of both allowed direct and indirect electron transitions. In the frequency range of 10^3-10^7 Hz the real Z' and imaginary Z'' part of the total impedance of pyroceramics/Al_2O_3/Al/V_2O_5/Al structure were studied. The applied direct bias leads to a considerable Z', as well as Z'' decrease. The analysis of the obtained dependencies is carried out by using the method of equivalent circuits.

(Received June 15, 2016; accepted June 7, 2017)

Keywords: Vanadium, Vanadium oxide, Nanocomposite structure, Oxide layer, Optical absorption spectra, Raman spectra, Impedance spectroscopy

1. Introduction

Recently, one can observe a growing interest in the study of nanocomposite structures properties and methods for their preparation. The nanodimensional structures of vanadium oxide are particularly promising because some oxides are metals, others are in a stable semiconducting state, the third have the semiconductor-metal phase transition (SMPT) [1]. V_2O_3 is the most studied oxide with SMPT at T = 168 K; VO_2 with SMPT at T = 340 K; V_2O5 has a stable semiconducting state.

Vanadium pentoxide V_2O_5 is widely studied because of its interesting electrochemical properties. It can be used as the catalyst [2], as the cathode in high efficiency lithium batteries [3], as a window for solar cells [4] and in electrochromic instruments [5], it may also be used for electronic and optical switches with low values of response times [6]. The results of V_2O_5 amorphous films studies are brought in [7]; but even the structure of freshly prepared amorphous films of V_2O_5 has not been studied, partly due to the difficulties related to conventional diffraction methods.

Many different methods of nanocomposite materials fabrication were reported. Along with a variety of vacuum and none vacuum methods of oxide layers obtaining a considerable interest presents the annealing in the oxygenated atmosphere of metal films, including vanadium [8] obtained by magnetron sputtering in a mixture of argon gas and oxygen by a procedure characterized by simplicity and high technological flexibility that provides ample opportunities for study of metal-oxygen interaction.

The nanodimensional composite structures created by the oxidation of vanadium films fabricated by vacuum deposition were studied in the given paper and some optical properties of the layers, the electrical properties were also investigated by impedance spectroscopy.

2. Experiment

For fabrication of nanodimensional vanadium oxide based composite structures the principles of self-organization and self-consistency was used. As it is noted in [9, 10], self-organized structures originate in open systems exposed to external inflow of matter having sufficient impact power for to ensure the system transition to the state away from equilibrium. These processes are initiated by thermal diffusion.

If we consider that V_2O_5 oxide is formed by accumulating of finely fractioned metal (vanadium) in an oxygen stream, and all derivatives of the lowest vanadium valences are easily transformed into V_2O_5 already at atmospheric oxygen exposure and temperature [2], then the oxidation of the fine vanadium layer will be formed around its atoms or conglomerates at the beginning of the V_2O_5 film plus all derivatives of lower vanadium valence oxides. The further annealing in air creates stable in time with a smooth surface nanostructure based on vanadium and its oxides. Nanodimensional films of 60-120 nm thick

vanadium pentoxide obtained by the method described in [11] were investigated in this study.

The pyroceramic plates, silica plates and glass plates covered by SnO_2 conductive layer, obtained by electrochemical deposition were used as substrates. To reduce the influence of the surface discontinuities of pyroceramics the 0.8μ÷ 1.0 μm thick Al_2O_3, SiO_2, Ta_2O_5 oxide film was deposited by electron-beam evaporation on its mirror surface.

The morphology of samples surface were studied using a VEGA TESCAN TS 5130 MM scanning electron microscope (SEM) and atomic force microscope AFM (SIS – scancontrol C). The Raman scattering was investigated at room temperature with a MonoVista CRS Confocal Laser Raman System in the backscattering geometry under the excitation by a MSL-III 532 nm (2.331 eV) DPSS laser. The spectra of optical reflection and transmission were measured on MDR-2 and Jasco-670 spectrometers at 300 K in spectral range of 200-1000 nm.

Impedance spectra were studied by using the Semiconductor Characterization System Keithley Model 4200-SCS with the amplitude of the *ac* signal of 10 mV in a frequency range $10^3 \div 10^7$ Hz for different values of the *dc* bias voltages U_{dc}= -1.0÷1.0 V with a step up to 0.1 V at room temperature.

3. Surface morphology

The nanodimensional structures on the basis of vanadium and its oxides were obtained on the surface of the pyroceramics substrate. The maximum free of impurities and structural imperfections and irregularities surface are required in nanotechnology. As studies have shown the glass-ceramic surface consists of sharp pyramidal needles of 50÷60 nm height (Fig. 1), which is comparable to the expected thickness of the nanocomposite film.

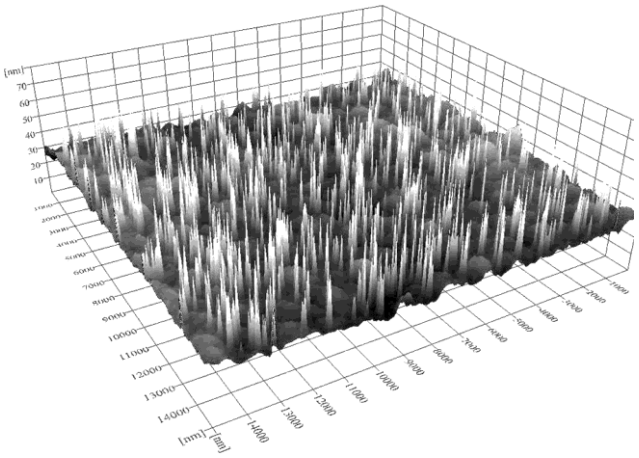

Fig.1. Three dimensional AFM images of the pyroceramics surface

When deposited to such a surface, the vanadium pentoxide is precipitated in the valleys between the peaks and forms a inhomogeneous layer across the surface. This fact leads to the formation of granular films (Fig. 2). The surface of the nanocomposite deposited on the pyroceramic substrate passivated by SiO_2 is shown in Fig. 3. There is a radical change in the morphology of the film surface - the surface becomes more uniform.

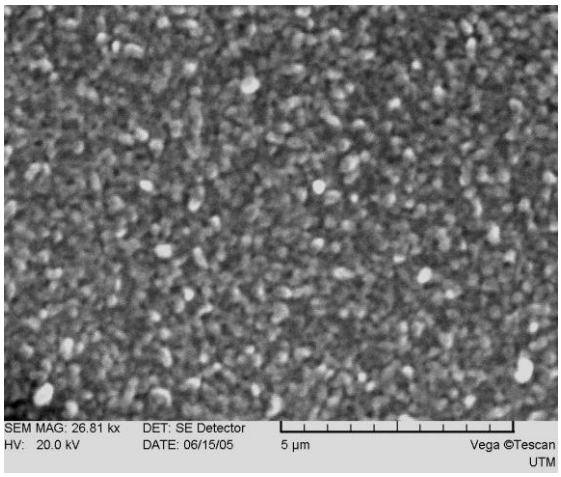

Fig. 2. SEM image of the V_2O_5 thin layer surface deposited on the initial surface of pyroceramics

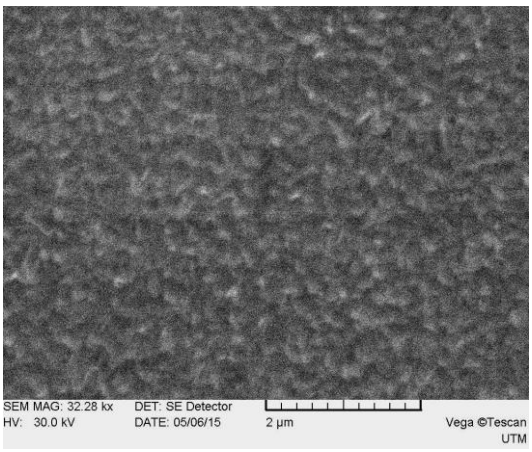

Fig. 3. SEM image of the V_2O_5 thin layer surface deposited on the pyroceramics substrate surface covered by SiO_2 layer

4. Raman Spectra

The Raman spectrum for the nanocomposite vanadium oxide (d~150 nm) film deposited on silica substrate is shown in Fig. 4.

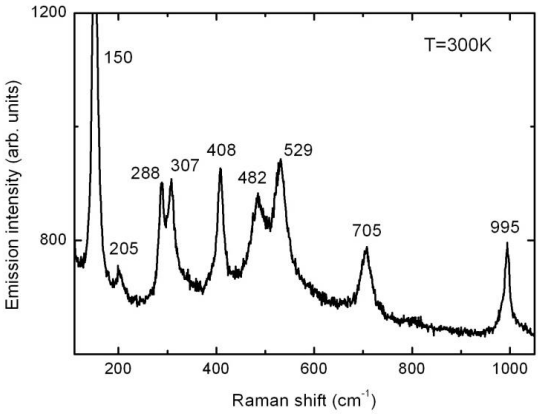

Fig.4. Raman scattering spectra of V_2O_5 based nanocomposite film

The positions of the Raman lines maxima obtained from Fig. 4 and compared with the data for V_2O_5 crystalline films from [12-14] are shown in Table 1.

The presence of distinct Raman scattering peaks indicates a high structural perfection of the resulting films, which may be polycrystalline ones with large crystallites. The Raman spectra of V_2O_5 films obtained on pyroceramics substrates passivated by Al_2O_3, Ta_2O_5, SiO_2 oxide and on glass substrates covered with SnO_2 layer, measured at room temperature are shown in Fig. 5. In the spectrum of the vanadium pentoxide film deposited on the passivation layer of tin oxide a Raman line characteristic for crystalline V_2O_5 is observed. Beside the line corresponding to VO_2 is observed in the spectra, the positions of their maxima are close to the known from the literature data [15]. These results allow to suppose, that during vanadium pentoxide formation the vanadium oxides of lower valence are formed, which do not appear in the Raman spectra due to their low concentration. It should be noted that the position of the maxima of some lines of these materials are identical or similar, what make them difficult to unambiguous interpretation.

Table 1. Raman shift of vanadium pentoxide

Nr.	Data from Fig,1. cm^{-1}	Data from the paper of S.-H. Lee et. al. [12], $см^{-1}$	Mode type [12-14]
1	150	142	layer vibration
2	205	194	layer vibration
3	288	283	V=O bending mode
4	307	303	V_3–O bending mode
5	408	405	V=O bending mode
6	482	487	V–O–V bending mode
7	529	530	V_3–O stretching mode
8	705	706	V_2–O stretching mode
9	995	1000	V=O stretching mode

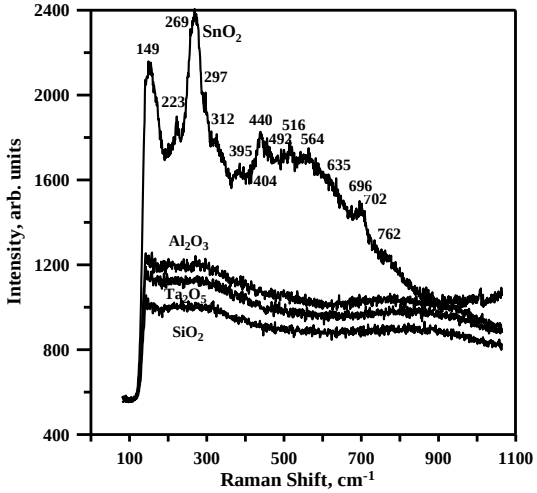

Fig. 5. Raman spectra of V_2O_5 films obtained on pyroceramics substrates passivated by Al_2O_3, Ta_2O_5, SiO_2 layer oxide and on glass with SnO_2 layer

On the Raman spectra of V_2O_5 films obtained on pyroceramics substrates passivated by Al_2O_3, Ta_2O_5, SiO_2 oxide do not appear clearly marked narrow lines (Fig. 5) which indicate their amorphous character.

Since the film obtained due to the particles self-organization during deposition process and heat treatments are locally inhomogeneous, and their thickness is about 60-120 nm, the Raman measurements are very difficult, and measurement of the polarization dependencies is impossible due to the varying orientation of the crystallites constituting the film. Another explanation could be the fact that we register the scattering of light in the layer of passivating oxide. Since the film of vanadium oxide is very thin the scattered light from the passivating layer is greater than the signal from the Raman scattering in vanadium oxide.

5. Optical properties

The absorption coefficient α has been determined from the expression:

$$T = \frac{(1-R)^2 e^{-\alpha d}}{1-R^2 e^{-2\alpha d}} \qquad (1)$$

where d~60 nm is the film thickness determined from the AFM data. T – the film transmittance, R - the film reflectance and α - absorption coefficient. The absorption spectrum, calculated by the formula (1), for a vanadium pentoxide V_2O_5 thin film deposited on a silica substrate and annealed at a temperature of 300°C during 1hr is shown in Fig. 6.

Good linearization of the experimental data was found at the spectrum presentation in the $(\alpha\hbar\omega)^2 = f(\hbar\omega)$ coordinates. The energy of direct allowed electron transition, determined from $(\alpha\hbar\omega)^2 = f(\hbar\omega)$ dependence (Fig.6) equals to 2.748 eV. From the absorption spectrum presented in $(\alpha\hbar\omega)^{1/2} = f(\hbar\omega)$ coordinates (Fig. 7) the energy of indirect electron transitions, involving a phonon with energy E_{ph} = 94.5 meV (762 cm^{-1})was determined, which equals to E_{ind} = 2.426 eV. The phonon wave number value ν_{ph} = 762 cm^{-1} is comparable with ν_{ph} = 705 cm^{-1} determined from the Raman spectra and related to the V_2-O stretching mode (Fig. 4, Table 1).

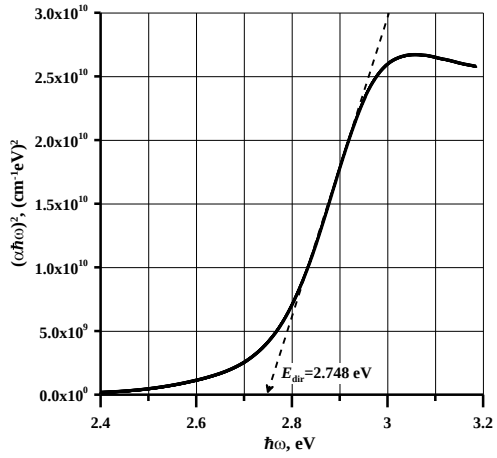

Fig. 6. The absorption spectrum of V_2O_5 thin film drawn in $(\alpha\hbar\omega)^2 = f(\hbar\omega)$ coordinates

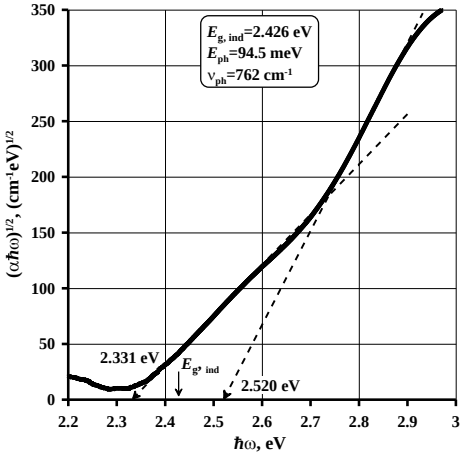

Fig.7. The absorption spectrum of V_2O_5 thin film drawn in $(\alpha\hbar\omega)^{1/2} = f(\hbar\omega)$ coordinates

6. Electrical proprieties

The real and imaginary parts of the impedance dependence on applied voltage of the pyroceramics/Al_2O_3/Al/V_2O_5/Al structure are given in (Fig. 8). As one can see from Fig.8 the increase of the applied to the studied structure voltage leads to a significant decrease in the Z '', and Z ' values and to Z' 'maxima displacement to a high frequency region. At the same time these changes do not depend on the sign of the applied voltage.

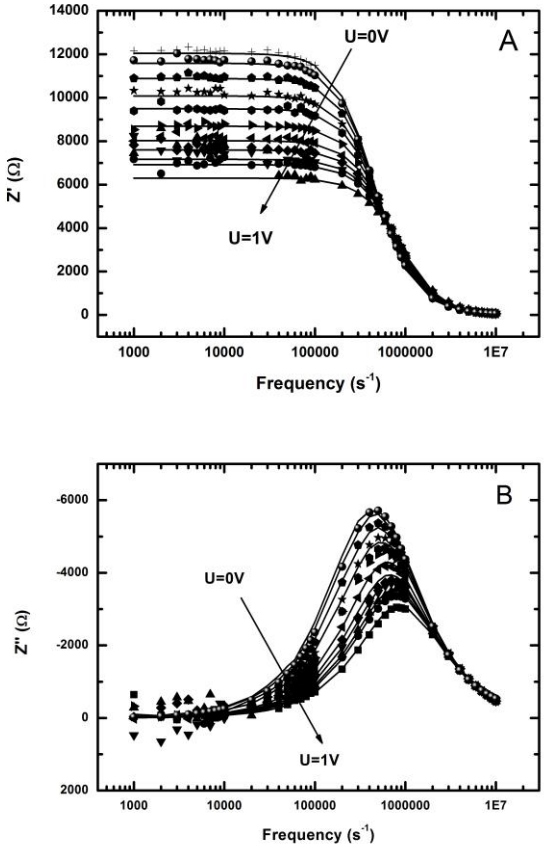

Fig. 8. Real (A) and imaginary (B) parts of the impedance measured at different applied voltages (circles) and theoretical curve (solid curve)

These dependencies allow to define an equivalent circuit for the studied structure. The best agreement between theory and experiment is obtained, when a equivalent circuit of the of R_pC_p parallel circuit and R_s resistor connected thereto in series, is used (Fig. 9).

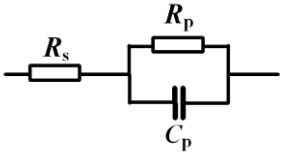

Fig. 9. The substitution equivalent circuit of pyroceramics/Al_2O_3/Al/V_2O_5/Al structure

The above said shows that the studied structure contains both conductive and dielectric (semiconductor) phase. We assume that the obtained films are composed of a vanadium metal grains coated by V_2O_5, which form large crystallites (Fig. 10.1), which in our opinion are of semiconducting (dielectric) phase. Between the grains the layers of a different chemical composition are created, which consists probably, from unreacted vanadium and lower order oxides and form a conductive phase (Fig. 10. 2).

According to the vanadium pentoxide film structure shown in Fig. 10 and its equivalent circuit (Fig. 9), resistor R_s corresponds to the resistance of the conductive phase (Fig. 10, 2). Resistor R_p takes into account the dielectric matrix resistance and is shunted by capacitor C_p, that corresponds to the geometrical capacitance of V_2O_5 grains and therefore practically is independent of the applied voltage (Fig. 11, C) [16].

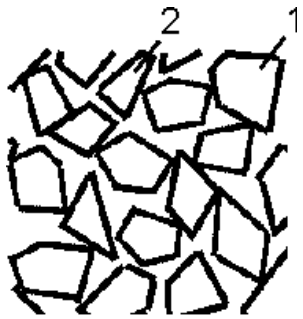

Fig. 10. The vanadium pentoxide film structure consists of a semiconductor phase (1) and the conductive phase (2)

However, it is necessary to notice that if the conductivity types of the interlayers and grain are different, than on the borders *p-n* junctions are localized, and this can be both homo- and heterojunctions. At the same type of the majority charge carriers the isotype heterojunctions or Schottky barriers can be formed. When applying an external bias voltage a part of these barriers is connected in the forward direction and the other in reverse. The influence of constant external field is due to the breakdown of a part of the barrier layers. The effect is more pronounced at low frequencies, since in this case a high resistance layers are formed in an alternating field. The breakdown of these layers leads to a significant decrease in resistance.

The resistance of barrier layers formed under the influence of the alternating field decreases with frequency increase, the depth of their depletion decreases. Accordingly, the contribution of barrier layers decreases, and the field in the sample is uniformly distributed over [17]. However, the grain boundaries influence effects, are dominant in the low-frequency range (1-1000 Hz), and the influence of crystallite is dominant in high frequency region. Therefore, in this case, at low bias voltages the influence of grain boundaries was not revealed and the main contribution into the impedance is brought by crystallites. The contribution of the effects associated with the influence of the boundaries begins to reveal and one can observe the shift of the Z'' and Z' spectral dependences in the high-frequency region and available for measuring low-frequency region with the increase of the applied voltage (Fig. 8).

Experimental data of impedance real and imaginary parts frequency dependences at different voltage bias and theoretical curves are given in Fig.8. The calculation was performed in accordance with the equivalent circuit (Fig. 9) according to the formulas (2-3):

$$Z' = R_s + \frac{R_p}{1+(\omega C_p R_p)^2}, \qquad (2)$$

$$Z'' = -\frac{\omega C_p R_p^2}{1+(\omega C_p R_p)^2}. \qquad (3)$$

As one can see from the graphs (Fig. 8) the experimental data and theoretical curves drawn according to formulas (2, 3) are in good agreement.

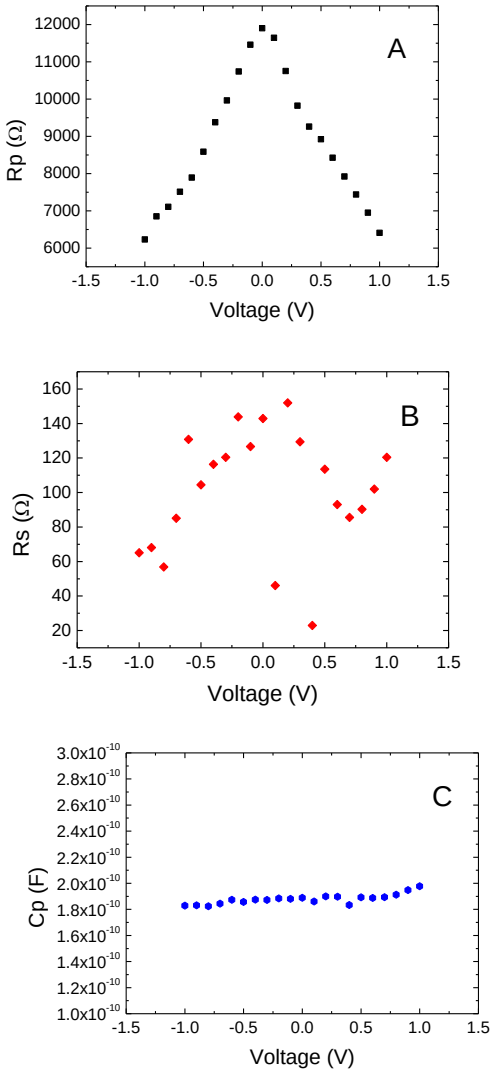

Fig.11. The values of equivalent circuit elements in dependence of the applied voltage

If to consider the voltage dependence of R_p resistance in the parallel *RC* circuit, it decreases with voltage increase irrespective of the sign of the applied voltage (Fig. 11 A). The series resistance R_s is changes randomly with voltage increase and is hard to identify a certain regularity in this case (Figure 11, B). C_p capacity is changes slightly with voltage increase and it can be considered independent on the voltage.

7. Conclusions

The choice of oxidation method of vanadium layer produced by thermal spraying, for obtaining of V_2O_5 oxide film results in the formation of a nanoscale composite structure, wherein the matrix consists of V_2O_5 crystals coarse-separated by mixtures of low-valence vanadium oxide (the dispersed phase).

According to Raman spectroscopy results the thin film structure obtained on quartz corresponds to the α-V_2O_5 orthorhombic phase.

Analysis of the optical properties of vanadium pentoxide thin films allowed to reveal energies of the electron transitions: E_{ind}=2.426 eV for the indirect transition , with the participation of phonons with energy of E_{ph} = 94.5 meV (ν_{ph} = 762 cm^{-1}) and E_{dir} = 2.748 eV for the allowed direct transition.

According to impedance spectroscopy there were established the structural features of the vanadium pentoxide film, which allowed to determine its equivalent circuit diagram in which resistor R_s corresponds to the resistance of the conductive phase, resistor R_p is related to the resistance of dielectric matrix, and C_p capacitance corresponds to the geometrical capacitance of V_2O_5 grains. The dependence of these parameters on the bias voltage was determined.

Acknowledgments

This research was supported by the STCU Project nr. 5808 and Institutional project nr. 15.817.02.34A.

Referencies

[1] W. Bruchner, H. Opperman, W. Reichelt et. al, Vanadium oxide, Akademie Verlag, Berlin (1983).
[2] R. Ramirez, B. Casal, L. Utrera, E. Ruiz-Hitzky, J. Phys. Chem. **94,** 8965 (1990).
[3] H. K. Park, W. H. Smyrl, M. D. Ward, J. Electrochem. Soc. **142**, 15 (1995).
[4] C. R. Aita, Y.-L.Liu, M. L. Kao, S. D. Hansen, J. Appl. Phys. **60**(2), 749 (1986).
[5] S. F. Cogan, N. M. Nguyen, S. J. Perrotti, R. D. Rauh, J. Appl. Phys. **66**(3), 1333 (1989).
[6] G. S. Nadkarni, V. S. Shirodkar, Thin Solid Films **105**, 115 (1983).
[7] Y. Dimitriev, V. Dimitrov, M. Arnaudov, D. Topalov, J. Non-Cryst. Solids **57**, 147 (1983).
[8] K. Sieradska, D. Wojcieszak, D. Kaczmarek, J. Domaradzki, G. Kiriakidis, E. Aperathitis, V. Kambilafka, F. Placido, Sh. Son, Optica Applicata, **XLI** (2), 463 (2011).
[9] G. Nicolos, N. Prigojin, Self-organization in nonequilibrium systems, Mir, Moskow (1979).
[10] I. N. Serov, V. A. Jabarev, V. N. Margolin, Fizica i himia stecla **29**(2), 242 (2003).
[11] V. Prilepov, P. Gasin, A. Chirita, V. Midoni, D. Spoiala, P. Ketrush, J. Optoelectron. Adv. M. **16**(1-2), 232 (2014).
[12] Se-Hee Lee, M. Hyeonsik Cheong, Maeng Je Seong, C. Ping Liu, Edwin Tracy, Angelo Mascarenhas, J. Roland Pitts, Stayen K. Deb, Solid State Ionics **165,** 111 (2003).
[13] A. Chakrabarti, K. Hermann, R. Druzinic, M. Witko, F. Wagner, M. Petersen, Physical Review B **59**(16), 10583 (1999).
[14] C. Julien, G. A. Nazri, O. Bergstrom, Phys. Status Solidi **B 201**, 319 (1997).
[15] V. S. Vihnin. I. N. Goncharuc, V. I. Davydov et al. Solid State Physics **37**(12), 3580 (1995).
[16] N. A. Poklonsky, N. I. Gorbaciuk, Fundamentals of impedance spectroscopy of composites, Minsk (2015).
[17] P. T. Oreshkin, Physics of semiconductors and dielectrics, Mir, Moskow (1976).

*Corresponding author: compovx@mail.ru